Cardiovasc Intervent Radiol (2012) 35:97–104
DOI 10.1007/s00270-011-0118-x

CLINICAL INVESTIGATION

Comparing the Detectability of Hepatocellular Carcinoma by C-Arm Dual-Phase Cone-Beam Computed Tomography During Hepatic Arteriography With Conventional Contrast-Enhanced Magnetic Resonance Imaging

Romaric Loffroy · MingDe Lin · Pramod Rao · Nikhil Bhagat · Niels Noordhoek · Alessandro Radaelli · Järl Blijd · Jean-François Geschwind

Received: 1 October 2010 / Accepted: 24 January 2011 / Published online: 17 February 2011

Abstract
Purpose To evaluate the sensitivity of dual-phase cone-beam computed tomography during hepatic arteriography (CBCTHA) for the detection of hepatocellular carcinoma (HCC) by comparing it with the diagnostic imaging "gold standard": contrast-enhanced magnetic resonance imaging (CE-MRI) of the liver.
Materials and Methods Eighty-eight HCC lesions (mean diameter 3.9 ± 3.3 cm) in 20 patients (13 men, mean age 61.4 years [range 50 to 80]), who sequentially underwent baseline diagnostic liver CE-MRI and then underwent early arterial- and delayed portal venous-phase CBCTHA during drug eluting-bead transarterial chemoembolization, were evaluated. Dual-phase CBCTHA findings of each tumor in terms of conspicuity were compared with standard CE-MR images and classified into three grades: optimal, suboptimal, and nondiagnostic.
Results Seventy-seven (mean diameter 4.2 ± 3.4 cm [range 0.9 to 15.9]) (93.9%) of 82 tumors were detected. Sensitivity of arterial-phase (71.9%) was lower than that of venous-phase CBCTHA (86.6%) for the detection of HCC lesions. Of the 82 tumors, 33 (40.2%) and 52 (63.4%), 26 (31.7%) and 19 (23.2%), and 23 (28%) and 11 (13.4%) nodules were classed as optimal, suboptimal, and nondiagnostic on arterial- and venous-phase CBCTHA images, respectively. Seventeen (73.9%) of the 23 tumors that were not visible on arterial phase were detected on venous phase. Six (54.5%) of the 11 tumors that were not visible on venous phase were detected on arterial phase.
Conclusions Dual-phase CBCTHA has sufficient image quality to detect the majority of HCC lesions compared with the imaging "gold standard": CE-MRI of the liver. Moreover, dual-phase CBCTHA is more useful and reliable than single-phasic imaging to depict HCC nodules.

Keywords Hepatocellular carcinoma · C-arm cone-beam CT · Angiography · Transarterial chemoembolization · Drug eluting-beads · Magnetic resonance imaging

Introduction

Hepatocellular carcinoma (HCC) is the third most common cause of cancer death worldwide [1]. The prognosis remains poor because most cases are still not diagnosed until the disease is already in an advanced stage [2]. The exact number and the distribution of tumor nodules are crucial for allocating these patients to adequate treatment regimens [3, 4]. Transarterial chemoembolization (TACE) is one the effective therapeutic options for inoperable HCC lesions [5–7]. However, angiography frequently cannot demonstrate HCC lesions because of their small size or decreased hypervascularity. This often results in TACE being reluctantly performed to a relatively large liver area because of difficulty in identifying the tumor and its feeding blood vessels. Recently, C-arm cone-beam computed tomographic (CBCT) technology using a flat-panel detector has emerged as a useful tool in conjunction with

R. Loffroy (✉) · P. Rao · N. Bhagat · J.-F. Geschwind
Russell H. Morgan Department of Radiology and Radiological Science, Division of Vascular and Interventional Radiology, Johns Hopkins Hospital, Baltimore, MD, USA
e-mail: romaric.loffroy@gmail.com

M. Lin
Clinical Informatics, Interventional, and Translational Solutions, Philips Research North America, Briarcliff Manor, NY, USA

N. Noordhoek · A. Radaelli · J. Blijd
Department of Biomedical Engineering, Philips Healthcare, Best, The Netherlands

standard digital subtraction angiography (DSA) for the detection of HCC lesions during TACE procedures [8–10]. However, to date, no study has compared the diagnosis capability of CBCT during hepatic arteriography (CBCTHA) with that of the diagnostic imaging "gold standard," conventional contrast-enhanced magnetic resonance imaging (CE-MRI) of the liver, for the detection of HCC nodules. A recent study showed that acquiring contrast-enhanced CBCT images during early arterial and delayed portal venous tumor enhancement phases provides superior liver tumor conspicuity than imaging a single phase alone [11]. To acquire the two phases, all current commercially available CBCT systems necessitate two separate contrast-enhanced scans for visualization of tumor feeding vessels and parenchymal staining. This increases the procedural time and total injected volume of contrast. In this study, dual-phase CBCT imaging during hepatic arteriography is used where only one contrast agent injection is needed [12]. The purpose of this study was to retrospectively evaluate the detectability of HCC nodules by dual-phase CBCTHA during drug eluting-bead TACE (DEB-TACE) compared with that by preintervention conventional CE-MRI of the liver.

Materials and Methods

Patient Study Selection

This single-institution, retrospective study was compliant with the Health Insurance Portability and Accountability Act and was approved by the Institutional Review Board. All patients provided informed consent before inclusion in the study. The diagnosis of HCC was confirmed by biopsy or by typical radiologic findings in addition to an increased serum alpha-fetoprotein level > 400 ng/mL. All candidates for DEB-TACE were evaluated and treated for unresectable HCC after discussion at our institution's multidisciplinary liver conference. Eligibility criteria for DEB-TACE were as follows: Eastern Cooperative Oncology Group (ECOG) performance status ≤ 2; Child-Pugh classification A or B; focal or multifocal hepatic malignancy; absent or traces ascites; albumin >2.5 g/dL; alanine aminotransferase and aspartate aminotransferase <5 times the upper normal limit; total serum bilirubin <3.0 mg/dL; serum creatinine <2.0 mg/dL; platelet count $\geq 50{,}000/\text{mm}^3$; international normalized ratio (INR) ≤ 1.5; left ventricular ejection fraction $\geq 50\%$; and no contraindications to MRI.

Between March 2009 and March 2010, dual-phase CBCTHA was performed in 27 patients with HCC during DEB-TACE. The patient selection criteria for the present study were as follows: (1) patients with <10 nodular HCC lesions; (2) patients who sequentially underwent preintervention diagnostic CE-MRI of the liver and then dual-phase CBCTHA immediately before DEB-TACE; and (3) patients who had not undergone previous therapy for HCC, including conventional lipiodol or DEB-TACE, other than liver resection and complete occlusion of the portal venous system. Of the 27 patients, 20 met these criteria. There were 13 men and 7 women with a mean patient age of 61.4 ± 11.4 years [range 50 to 80). In total, 88 tumors (mean per patient 4.4; [range 1 to 10) with a mean diameter 3.9 ± 3.3 cm ([range 0.7 to 15.9) were demonstrated on pre–DEB-TACE CE-MRI of the liver. Table 1 lists the demographic data for this 20-patient cohort. The majority of patients had multifocal HCC with preserved underlying liver function (Child-Pugh class A disease). Most patients (60% [12 of 20]) had cirrhosis, and 45% were classified as Barcelona Clinic Liver Cancer (BCLC) grade C (A/B/C/D = 2/8/9/1, respectively). Table 1 lists baseline characteristics of patients before treatment.

Conventional MRI Technique

All patients underwent baseline MRI approximately 1 month before the DEB-TACE procedure and were imaged using a 1.5-T MRI unit (CV/I; GE Medical Systems, Milwaukee, WI) with a phased-array torso coil. The imaging protocol included the following: (1) axial T2-weighted fast spin-echo images (TR/TE; 5000/100 msec; matrix size 256×256; slice thickness 8 mm; interslice gap 2 mm; and receiver bandwidth 32 kHz), (2) axial single-shot breath-hold gradient-echo diffusion-weighted echo-planar images (TR/TE; 5000 to 6500/110 msec; matrix size 128×128; slice thickness 8 mm; interslice gap 2 mm; b-value 500 s/mm^2; and receiver bandwidth 64 kHz), and (3) axial breath-hold unenhanced and contrast-enhanced (0.1 mmol/kg intravenous gadodiamide [Omniscan; Amersham, Princeton, NJ]) T1-weighted three-dimensional (3D) fat-suppressed spoiled gradient-echo images (TR/TE; 5.1/1.2 ms; field of view 320 to 400 mm^2; matrix size 192×160; slice thickness 4 to 6 mm; receiver bandwidth 64 kHz; and flip angle 15°) in the arterial and portal venous phases (20 and 70 seconds after intravenous contrast administration, respectively).

C-Arm Dual-Phase CBCT Technique

All patients underwent C-arm dual-phase CBCT imaging during hepatic arteriography before DEB-TACE therapy but after arteriograms of the celiac and superior mesenteric arteries. The imaging was performed using a commercially available angiographic system (Allura Xper FD20; Philips Healthcare, Best, The Netherlands). This system was equipped with the XperCT option, enabling C-arm CBCT

Table 1 Baseline characteristics of patients with HCC before treatment

Baseline characteristics	Value (*n* or mean ± SD)
Demographics	
No. of patients/no. of tumor lesions	20/88
Age (y)	61.4 ± 11.4
Sex (male/female)	13/7
Race (White/African-American/Hispanic/Other)	9/6/1/4
Etiology (alcohol/HCV/HBV/NASH/cryptogenic)	2/9/2/2/5
ECOG performance status (0/1/2/3/4)	13/6/1/0/0
Cirrhosis (present/absent)	12/8
Type (unifocal/multifocal/diffuse)	5/9/6
Portal vein thrombosis (yes/no)	6/14
Tumor size (cm)	3.9 ± 3.3
HCC staging	
Child-pugh class (A/B/C)	14/6/0
BCLC stage (A/B/C/D)	2/8/9/1
Okuda stage (I/II/III)	9/10/1
CLIP score (1/2/3/4)	7/7/5/1
Serum tests	
Basal AFP (ng/mL)	49,138 ± 205,333
<10	8
10–200	5
>200	7
Albumin (g/dL)	3.7 ± 0.7
Total bilirubin (mg/dL)	2.1 ± 3.9
AST (U/L)	125.3 ± 86.1
ALT (U/L)	104.8 ± 81.9
Alkaline phosphatase (U/L)	242.4 ± 297.9
INR	1.2 ± 0.8

HCV hepatitis C virus, *HBV* hepatitis B virus, *NASH* nonalcoholic steato-hepatitis, *CLIP* cancer of the liver Italian program, *AFP* alpha-feto-protein, *AST* aspartate aminotransferase, *ALT* alanine aminotransferase

acquisition and volumetric image reconstruction (Feldkamp back projection) [13]. For each CBCT scan, the area of interest was positioned in the system isocenter and during approximately 10 s, 312 projection images (30 frames/s) were acquired with the motorized C-arm covering a 200° clockwise arc at a 20°/s rotation speed. As the images were being acquired, the projections were transferred by way of fiber optic to the reconstruction computer to produce volumetric data. The two-dimensional projection images were reconstructed using Feldkamp back projection [13] into 3D volumetric images with an isotropic resolution of 0.98 mm for a 250 × 250 × 194–mm field of view (FOV) (matrix size 256 × 256 × 198). The dual-phase CBCT prototype feature modified the XperCT option to assure acquisition of two sequential, back-to-back CBCT scans so both early or arterial and delayed or portal venous phases are captured using only one contrast injection [12].

In this study, the two scans were triggered at 3 and 28 s after a selective single injection of undiluted contrast medium through a 3F coaxial microcatheter placed into the proper hepatic artery. The same contrast injection protocol was applied to all cases (amount 20 mL; rate 2 mL/s [Oxilan 300 mg I/mL; Guerbet LLC, Bloomington, IN]). The patients were instructed to be at end expiration apnea during each of the CBCT scans with free breathing between the arterial and venous phase scans. Oxygen was administered to patients during the procedure to minimize the discomfort of breath holding. One millimeter-thick CT-like axial images were obtained for observation of CBCT images.

Image Analysis

The imaging "gold standard" for HCC diagnosis is conventional CE-MRI. Dual-phase CBCTHA findings of each tumor in terms of conspicuity were classified into three grades compared with pre–DEB-TACE conventional CE-MRI of the liver: (1) optimal = the tumor was clearly detectable such as that in conventional CE-MRI; (2) suboptimal = the tumor was faintly detectable compared with conventional CE-MRI; and (3) nondiagnostic = the tumor could not be detected. Sensitivity of dual-phase CBCTHA

for the detection of HCC lesions was defined as any tumor classified as optimal or suboptimal. This classification was used separately for both arterial and venous phases of dual-phase CBCTHA. Sensitivity was calculated for arterial phase, venous phase, and biphasic CBCTHA after exclusion of HCC lesions that were outside of the FOV.

Two experienced radiologists, who did not participate in the procedures retrospectively, evaluated all CE-MR and dual-phase CBCTHA images by consensus on a commercial workstation (Philips), on which the observers could manually alter the window level and width of the images to optimize image contrast. Artifacts were defined as the presence of streak artifacts, and/or motion artifacts, and/or artifacts from the catheter placed in the hepatic artery.

Results

Dual-phase CBCTHA was performed in all patients (100%). Almost all dual-phase CBCTHA images had minimal to severe artifacts (Fig. 1). Furthermore, the contrast between the HCC lesion and the surrounding liver parenchyma on dual-phase CBCTHA images was usually less than that seen on CE-MR images.

Dual-phase CBCTHA demonstrated 59 of the 82 tumors that were inside the FOV on arterial phase and 71 of these 82 tumors on venous phase. Therefore, the sensitivity of dual-phase CBCTHA for the detection of HCC lesions was 71.9% and 86.6% for arterial and venous phases, respectively. In total, 77 (mean 4.2 ± 3.4 cm [range 0.9 to 15.9]) (93.9%) of 82 tumors were detected either on arterial or venous dual-phase CBCTHA images (Fig. 2). In other words, the overall sensitivity of dual-phase CBCTHA (93.9%) to detect HCC lesions was greater than that of single-phase CBCTHA alone (arterial 71.9% and venous 86.6%). Of the 82 tumors, 33 (mean 4.7 ± 3.2 cm [range 0.9 to 13.3]) (40.2%) and 52 (mean 4.5 ± 3.6 cm [range 0.9 to 15.9]) (63.4%) nodules were classed as optimal on arterial and venous phases, respectively. Twenty-six (mean 4.4 ± 4.1 cm [range 1.0 to 10.5]) (31.7%) and 19 (mean 4.3 ± 3.1 cm [range 1.0 to 10.1]) (23.2%) of nodules were classed as suboptimal on arterial and venous phases, respectively. Twenty-three (mean 2.4 ± 1.9 cm [range 0.7 to 10.1]) (28%) and 11 (mean 1.7 ± 0.9 cm [range 0.7 to 4.4]) (13.4%) nodules were classed as nondiagnostic on arterial and venous phases, respectively. Interestingly, among the 23 tumors inside the FOV that could not be detected on arterial-phase CBCTHA, 17 (73.9%) of them were detected on venous phase (Fig. 3). Among the 11 tumors inside the FOV that could not be detected on venous-phase CBCTHA, 6 (54.5%) of them were detected on arterial phase. Overall, 11 (mean 1.9 ± 1.0 cm [range 0.7 to 4.4]) (12.5%) of 88 tumors in 3 patients could not be detected either on arterial or on venous dual-phase CBCTHA images. The cause of nondetectability varied widely: Six tumors (mean 2.5 ± 1.1 cm [range 1.3 to 4.4]) located in the lateral and upper segments of the liver in 1 patient were outside of the FOV; three tumors (mean 1.6 ± 0.2 cm [range 1.4 to 1.7]) in another patient were not visible because of severe artifacts on both phases; and the remaining two tumors in 1 patient measured <1 cm in diameter (mean 0.8 ± 0.1 cm [range 0.7 to 0.9]). Overall,

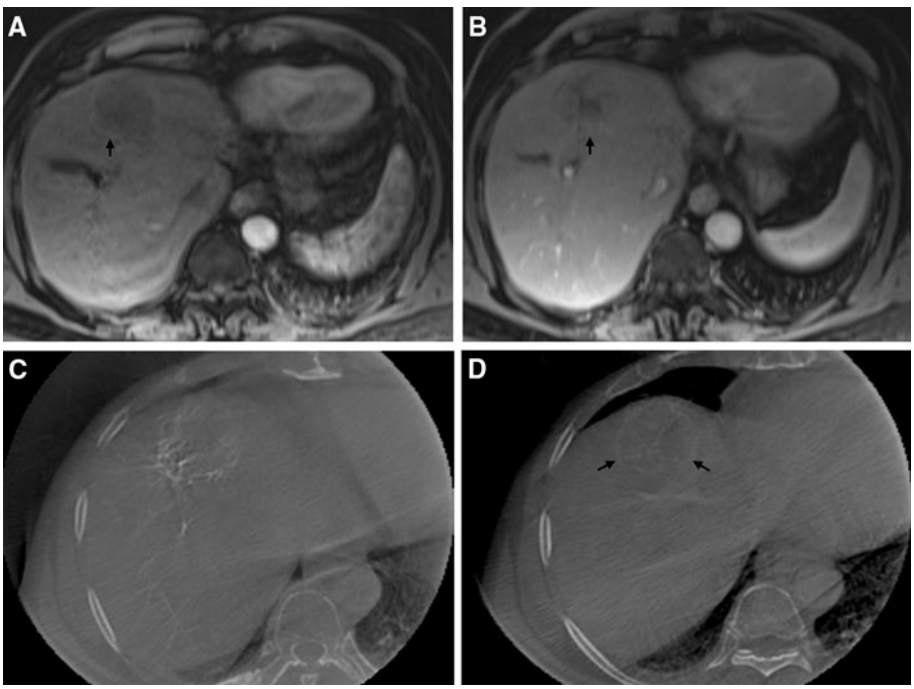

Fig. 1 A 77-year-old male patient with unifocal HCC (Child-Pugh score 5/class A). **A** Conventional CE-MR image shows a hypoattenuating mass in liver segment 8 in the arterial phase (*black arrow*). **B** Venous phase CE-MR image shows delayed tumor enhancement with central necrosis (*black arrow*). **C** Arterial phase dual-phase CBCTHA image shows the hypoattenuating mass. However, strong image artifacts from vessel filling are also seen. **D** Venous phase dual-phase CBCTHA image shows a sharply defined tumor area (*black arrows*) even if the contrast between the tumor and surrounding liver parenchyma is not optimal

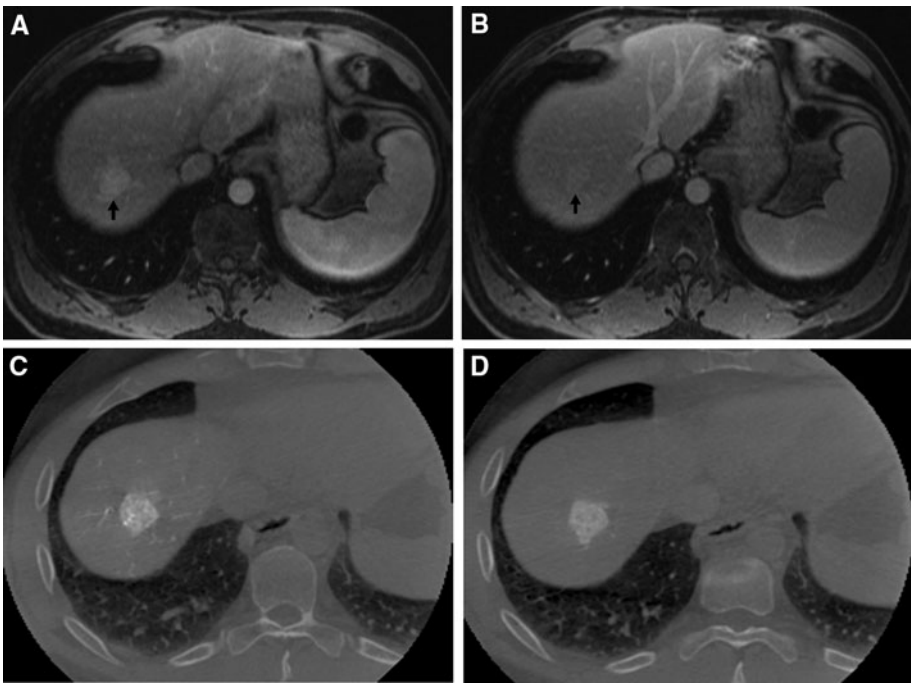

Fig. 2 A 50-year-old male patient with unifocal HCC (Child-Pugh score 5/class A). **A** Preintervention conventional CE-MR image at 20 s after intravenous contrast injection shows a hyperattenuating mass in the right liver dome (*black arrow*). **B** This mass becomes isointense to the healthy liver tissue on delayed CE-MR image at 70 s after contrast injection. **C** Arterial phase dual-phase CBCTHA image before injection of DEB clearly shows the tumor without any artifacts and matching with the MRI scans. **D** Note how the venous phase dual-phase CBCTHA image shows clear persistent tumor enhancement. In this case, the contrast between the tumor and surrounding liver parenchyma is greater than that seen on conventional CE-MRI

4 (6.7%) of 60 tumors >2 cm, 5 (20.8%) of 24 tumors >1 cm but <2 cm, and 2 (50%) of 4 tumors <1 cm were not detected on arterial or on venous phase. In addition, the 23 tumors inside the FOV classed as nondiagnostic on the arterial phase CBCTHA images were not detected because of severe artifacts ($n = 21$) and small size < 1 cm ($n = 2$) in 6 and 1 patients, respectively. The 11 tumors inside the FOV classed as nondiagnostic on venous phase images were not detected because of severe artifacts ($n = 9$) and small size <1 cm ($n = 2$) in 4 and 1 patients, respectively. Dual-phase CBCTHA did not detect any nodular lesions suspected of being HCC other than those already shown on pre-DEB-TACE conventional CE-MRI of the liver.

Discussion

C-arm CT technology allows for the acquisition of a 3D dataset generated from one rotational run with the use of cone-beam CT principles. Compared with conventional DSA, CBCT imaging can provide additional useful information for patients undergoing TACE [8, 10, 11, 14, 15]. Similarly, early and on-going clinical experience has demonstrated that CBCT using dual-phase imaging can provide better information than DSA for TACE and, occasionally, conventional CT or MRI regarding the number and distribution of tumors because of the hyperacute nature of the arterial contrast medium bolus. This can result in more effective and safer interventions. This technology has been introduced in interventional procedures [16–19]. However, few reports exist concerning the detectability of CBCT for liver tumors [8, 10, 20], and none of them has compared the diagnostic capability of CBCT with that of the diagnostic imaging "gold standard" of conventional CE-MRI. Furthermore, all current commercially available CBCT systems are single-phase CBCT systems.

In the present study, we evaluated the diagnostic potential of dual-phase CBCTHA for the detection of HCC lesions compared with conventional CE-MRI of the liver. CBCTHA depicted approximately 93.9% of HCC nodules in the present study, including 26 and 19 suboptimal lesions at the arterial and venous phases, respectively. Even if spatial and contrast resolution of dual-phase CBCTHA is inferior to that of conventional CE-MRI, we found that dual-phase CBCTHA had sufficient image quality to detect the majority of HCC lesions. Notably, dual-phase acquisition allowed improved detectability of HCC lesions compared with single-phase studies that were evaluated separately.

Miyayama et al. [8] reported that single-phase CBCT images depicted approximately 89% of HCCs; however, in our study the detectability of HCCs at dual-phase CBCTHA was 93.9%. Four factors may contribute to explain this discrepancy. First, the imaging protocols were different. For CBCTHA, Miyayama et al. [8] injected 40 ml contrast material at a rate of 3 ml/s and began scanning 25 s after the start of contrast injection. Under our dual-phase CBCTHA protocol, we injected 20 ml contrast material at a rate of 2 ml/s and start scanning 3 and 28 s after the start of contrast injection, respectively. Although it may not achieve sufficient liver enhancement, the

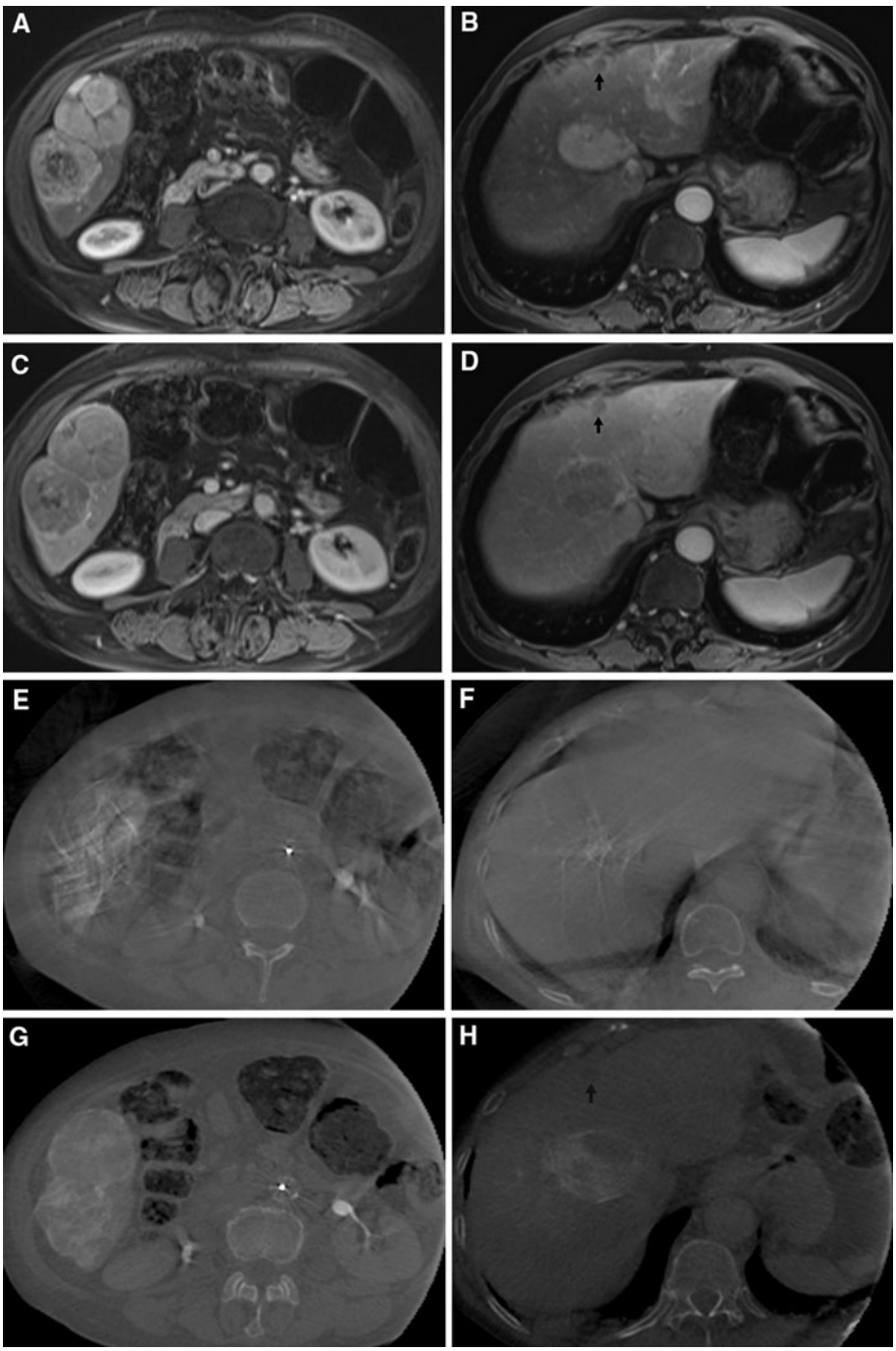

Fig. 3 A 77-year-old female patient with multifocal HCC (Child-Pugh score 5/class A). **A** and **B** Arterial phase CE-MR images at two axial slice levels show two partially necrotic enhancing masses in liver segment 6, at the inferior tip of the right hepatic lobe; one more enhancing tumor in liver segment 5; and a small subcapsular hypoattenuating mass in liver segment 4 (*black arrow* in [**B**]). **C** and **D** Venous phase CE-MR images at the same corresponding axial slice levels show washout of the three largest lesions and persistent hypointense feature of the smallest one (*black arrow* in [**D**]). **E** and **F** Arterial phase dual-phase CBCTHA images immediately before drug eluting bead-embolization are nondiagnostic because of severe motion and streak artifacts. **G** and **H** In contrast, venous phase dual-phase CBCTHA images are optimal and clearly show tumor parenchymal space for all lesions, even the smallest one (*black arrow* in [**H**]) matching with the CE-MR images

protocol used in this study decreased the amount of contrast medium required while yielding excellent tumor feeding vessel visualization. Second, the "gold standard" for diagnosis of HCC in the study by Miyayama et al. [8] was conventional CT during arterial portography (CTAP) findings. In our study, the "gold standard" imaging modality was conventional CE-MRI of the liver. Even if some reports exist describing the excellent image quality of CTAP for detecting HCC lesions [21–23], we consider that CE-MRI has better capacity to detect HCC lesions that require treatment. Consequently, the use of CTAP as gold standard could have led to a lower sensitivity for detecting HCCs in the study by Miyayama et al. [8] compared with CE-MRI. Third, Miyayama et al. [8] included the lesions located in the outside of FOV for calculation of sensitivities. Last, they used single-phase CBCTHA. These considerations might explain that the sensitivity of CBCTHA for detecting HCC lesions in our study was slightly greater than that of Miyayama et al. [8]. In the same way, Meyer et al. [11] evaluated the diagnostic accuracy and scan

coverage of flat-detector C-arm CT compared with that of biphasic MDCT for depicting malignant hepatic lesions in patients with hypervascular liver tumors before they underwent TACE. In this study, biphasic arterial and portal venous C-arm CT was performed and showed a greater sensitivity, ranging from 97 to 100%, for the detection of malignant liver lesions. However, the liver could not be visualized completely in two thirds of the patients because of incomplete scan coverage on C-arm CT. Furthermore, the main drawback of the scan technique used in this study was the need for positioning the catheter in two different arteries: the celiac trunk and the superior mesenteric artery.

Our study demonstrates several potential clinical advantages of dual-phase CBCTHA. The novelty of the technology presented in this article is the possibility for tumor imaging at both early arterial (tumor feeding vessel enhancement) and delayed venous (tumor parenchymal enhancement) phases using only one intra-arterial injection of contrast medium. This improvement decreases the use of iodinated contrast medium by 50% for the CBCT component of the interventional procedure. Furthermore, the simultaneous display of both phases side by side and with cine through the slices allows for direct visual comparison between the two phases. The former visual comparison (arterial *vs*. venous) could provide an idea of the vascular density of the tumor in relation to the feeding vessel. In addition, dual-phase CBCT acquisition offers more security and reliability in the detection of HCCs in obtaining at least one phase of good quality in the majority of patients, in case of significant artifacts on the other phase, as shown in our study. Last, the x-ray effective dose from CBCT imaging is significantly less than a typical abdomen scan using diagnostic multi-detector CT, even when two CBCT scans are performed [12, 24].

Limitations

There are some limitations to the present study. First, there was an obvious bias in patient recruitment because previous MRI results suggested HCC in all patients before they entered the study protocol. Furthermore, the majority of patients were diagnosed in an intermediate stage with multilocular disease and sometimes with large tumor nodules, which might have biased sensitivity. Second, histological confirmation was not obtained in all tumors. In most cases, only one representative lesion was examined pathologically, meaning that the diagnosis of additional tumor nodules relied on imaging only. However, we considered that advances in imaging modalities, especially MRI, have facilitated the establishment of HCC diagnosis without biopsy. Third, angiography was performed before dual-phase CBCT in all cases. This may decrease the contrast between HCC lesions and surrounding liver parenchyma on dual-phase CBCTHA images because of the retention of previously injected contrast material in the tumor interstitium. Last, the DEB-TACE procedure was performed on average 1 month after diagnostic CE-MRI of the liver in all patients. This interval could have led to the development of new HCC lesions and potentially to dual-phase CBCTHA depiction of HCC nodules that were not present on CE-MR images. However, in the present study, dual-phase CBCTHA did not detect any nodular lesions suspected of being HCC other than those already shown on conventional CE-MRI of the liver. Despite these limitations, the data demonstrate that diagnostic results depend considerably on the biphasic CBCTHA imaging protocol. Furthermore, dual-phase CBCTHA has a benefit compared with CE-MRI in that CBCTHA imaging can be performed during the TACE procedure with minimal additional effort than x-ray DSA and fluoroscopy. This can provide live-image feedback on the DEB-TACE delivery catheter positioning, drug delivery amount, and embolization success.

We estimate that dual-phase CBCTHA failed to depict HCC in our study essentially because (1) artifacts from the contrast-filled catheter placed in the hepatic artery and/or motion artifacts attributable to inadequate breath-holding may have decreased image quality and made it difficult to detect lesions, especially small HCC nodules; (2) the injection protocol was suboptimal; (and 3) some patients exceeded the FOV. Our technique continues to evolve as we gain more experience with this novel dual-phase CBCT application. Currently, many technical advances are under study for helping us to minimize image artifacts, and to optimize the contrast injection and imaging protocol, including: (1) shortening the acquisition scan time while emphasizing patient compliance for breath-holds; (2) improving postacquisition image processing to provide motion compensation and metal artifact correction; (3) using diluted contrast media to potentially decrease artifacts in the arterial phase; and (4) decreasing source-to-detector distance during scanning to resolve FOV problems. More specifically, optimization of contrast material administration is probably important to avoid contrast-related hardening artifacts. Indeed, we did not use diluted contrast material in our study, and we observed a large number of compromising artifacts. Even if a large proportion of them were due to motion rather than suboptimal contrast injection protocol, streak artifacts were also frequent and have probably led to heterogeneous contrast uptake in some patients, underlining the importance of contrast dilution.

In conclusion, dual-phase CBCTHA has sufficient quality to detect the majority of HCC lesions compared with gold standard CE-MRI of the liver, even if the image quality is not always optimal. Moreover, we consider

dual-phase CBCTHA more useful and reliable than single-phase to depict HCC nodules.

Acknowledgments This study was funded by the French Society of Radiology and supported by a Grant from Philips Research North America, Briarcliff Manor, NY.

Conflict of Interest The authors declare that they have no conflict of interest.

References

1. El-Serag HB, Rudolph KL (2007) Hepatocellular carcinoma: epidemiology and molecular carcinogenesis. Gastroenterology 132:2557–2576
2. Takayasu K, Arii S, Ikai I et al (2006) Prospective cohort study of transarterial chemoembolization for unresectable hepatocellular carcinoma in 8510 patients. Gastroenterology 131:461–469
3. Mazzaferro V, Regalia E, Doci R et al (1996) Liver transplantation for the treatment of small hepatocellular carcinomas in patients with cirrhosis. N Engl J Med 334:693–699
4. Yamashita Y, Mitsuzaki K, Yi T et al (1996) Small hepatocellular carcinoma in patients with chronic liver damage: prospective comparison of detection with dynamic MR imaging and helical CT of the whole liver. Radiology 200:79–84
5. Llovet JM, Real MI, Montana X et al (2002) Barcelona Liver Cancer Group. Arterial embolisation or chemoembolisation versus symptomatic treatment in patients with unresectable hepatocellular carcinoma: a randomised controlled trial. Lancet 359:1734–1739
6. Lo CM, Ngan H, Tso WK et al (2002) Randomized controlled trial of transarterial lipiodol chemoembolization for unresectable hepatocellular carcinoma. Hepatology 35:1164–1171
7. Llovet JM, Bruix J (2003) Systematic review of randomized trials for unresectable hepatocellular carcinoma: chemoembolization improves survival. Hepatology 37:429–442
8. Miyayama S, Matsui O, Yamashiro M et al (2009) Detection of hepatocellular carcinoma by CT during arterial portography using a cone-beam CT technology: comparison with conventional CTAP. Abdom Imaging 34:502–506
9. Kakeda S, Korogi Y, Ohnari N et al (2007) Usefulness of cone-beam CT with flat panel detectors in conjunction with catheter angiography for transcatheter arterial embolization. J Vasc Interv Radiol 18:1508–1516
10. Miyayama S, Yamashiro M, Okuda M et al (2009) Usefulness of cone-beam computed tomography during ultraselective transcatheter arterial chemoembolization for small hepatocellular carcinomas that cannot be demonstrated on angiography. Cardiovasc Intervent Radiol 32:255–264
11. Meyer BC, Frericks BB, Voges M et al (2008) Visualization of hypervascular liver lesions during TACE: Comparison of angiographic C-arm CT and MDCT. AJR Am J Roentgenol 190:W263–W269
12. Lin M, Loffroy R, Noordhoek N, et al. (2010) Evaluating tumors in transcatheter arterial chemoembolization (TACE) using dual-phase cone-beam CT. Minim Invasive Ther Allied Technol [Epub ahead of print]
13. Feldkamp LA, Davis LC, Kress JW (1984) Practical cone-beam algorithm. J Opthalmol Soc Am A 1:612–619
14. Wallace MJ (2007) C-arm computed tomography for guiding hepatic vascular interventions. Tech Vasc Interv Radiol 10:79–86
15. Wallace MJ, Kuo MD, Glaiberman C, Binkert CA, Orth RC, Soulez G (2008) Three-dimensional C-arm cone-beam CT: applications in the interventional suite. J Vasc Interv Radiol 19:799–813
16. Hirota S, Nakao N, Yamamoto S et al (2006) Cone-beam CT with flat-panel-detector digital angiography system: Early experience in abdominal interventional procedures. Cardiovasc Intervent Radiol 29:1034–1038
17. Orth RC, Wallace MJ, Kuo MD (2008) C-arm cone-beam CT: general principles and technical considerations for use in interventional radiology. J Vasc Interv Radiol 19:814–821
18. Georgiades CS, Hong K, Geschwind JF et al (2007) Adjunctive use of C-arm CT may eliminate technical failure in adrenal vein sampling. J Vasc Interv Radiol 18:1102–1105
19. Deschamps F, Solomon SB, Thornton RH, et al. (2010, April 14) Computed analysis of three-dimensional cone-beam computed tomography angiography for determination of tumor-feeding vessels during chemoembolization of liver tumor: A pilot study. Cardiovasc Intervent Radiol [Epub ahead of print]
20. Miyayama S, Yamashiro M, Okuda M, Yoshie Y, Nakashima Y, Ikeno H et al (2011) Detection of corona enhancement of hypervascular hepatocellular carcinoma by C-arm dual-phase cone-beam CT during hepatic arteriography. Cardiovasc Intervent Radiol 34(1):81–86
21. Matsui O, Takashima T, Kadoya M et al (1985) Dynamic computed tomography during arterial portography: the most sensitive examination for small hepatocellular carcinomas. J Comput Assist Tomogr 9:19–24
22. Matsui O, Kadoya M, Kameyama T et al (1991) Benign and malignant nodules in cirrhotic livers: distinction based on blood supply. Radiology 178:493–497
23. Matsui O, Ueda K, Kobayashi S et al (2002) Intra- and perinodular hemodynamics of hepatocellular carcinoma: CT observation during intra-arterial contrast injection. Abdom Imaging 27:147–156
24. Racadio J, Yoshizumi T, Toncheva G, Stueve D, Anderson-Evans C, Frush D (2008) Radiation dosimetry evaluation of C-arm cone beam CT for pediatric interventional radiology procedures: a comparison with MDCT. RSNA, Chicago, IL